Available online at www.sciencedirect.com
ScienceDirect
Electrochimica Acta 52 (2007) 4197–4201
ELECTROCHIMICA Acta
www.elsevier.com/locate/electacta

Synthesis and electrochemical properties of $Sn_{87}Co_{13}$ alloys by $NaBH_4$ and sodium naphthalenide reduction methods

Hyunjung Kim, Jaephil Cho *

Department of Applied Chemistry, Kumoh National Institute of Technology, Gumi 730-701, Republic of Korea

Received 13 September 2006; received in revised form 22 November 2006; accepted 24 November 2006
Available online 20 December 2006

Abstract

$Sn_{87}Co_{13}$ alloys are prepared by two different reduction methods and characterized by X-ray diffraction (XRD), transmission electron microscopy (TEM), and electrochemical cycling. One method, using $NaBH_4$ as a reducing agent, obtains aggregated particles with particle sizes from 20 to 200 nm. The second method, using sodium naphthalenide as a reducing agent, shows a well-dispersed nanoalloy coated with amorphous carbon, with a particle size of 15 nm. Although electrochemical results shows that the charge capacity of the two alloys is quite similar, 662 mAh/g, the capacity retention of the nanoalloy prepared using sodium naphthalenide was 427 mAh/g, which is two times higher after 30 cycles than the bulk analogue obtained using $NaBH_4$. This is due to the uniform particle size and amorphous carbon layer that effectively reduces anisotropic volume expansion and also minimizes particle aggregation and pulverization that causes a direct electrical disconnection with the copper current collector.

Keywords: $Sn_{87}Co_{13}$; $NaBH_4$; Sodium naphthalenide; Anode; Li battery; Capacity; Irreversible capacity

1. Introduction

The maximum utilizable capacity of a 18650 size cylindrical Li-ion cell is about 2800 mAh/g when a charge cut-off voltage of 4.4 V is used. The capacity of natural graphite is ~365 mAh/g. In order to increase the capacity of the cell beyond 2800 mAh, metal-based anode materials are used, and Sn and Si alloys have been intensively investigated [1–8]. However, the significant volume changes that these alloys incur during lithium alloying and dealloying causes cracking and crumbling of the electrode material and, consequentially, a loss of electrical contact between particles. In order to reduce mechanical strain, particles of smaller size or consisting of active/inactive composites have been made and are shown to possess improved capacity retention [9–11]. In this regard, ball-milling methods have been widely investigated because the composite can be easily prepared [12–14].

Mechanically alloyed Sn–Fe–C and Ag–Fe–Sn or Sn–C composite have been reported, and, depending on the composition, a first charge capacity as high as 600 mAh/g can be obtained [13,15,16]. However, this method suffers from the disadvantages of poor control of particle size and poor dispersity of the active phase in the inactive matrix phase. On the other hand, a chemical reduction method using $NaBH_4$ has been reported [1,17–21]. Yang et al. report the synthesis of Sn–SnSb microcrystalline powders with a particle size <300 nm using $NaBH_4$ as a reducing agent, and relatively good reversibility of the Sn–SnSb composite with a value of about 360 mAh/g [1]. Wang et al. report that phenanthroline capped tin nanoparticles with a particle size <10 nm using $NaBH_4$ have a maximum reversible capacity of 434 mAh/g, but initial irreversible capacity was 36% [22]. Recently, Xie et al. reported that $CoSb_2$ nanoparticles are successfully made by solvothermal synthesis above 120 °C using $NaBH_4$, and the particle size was larger than 60 nm [18]. The first charge capacity was 672 mAh/g but showed a large irreversible capacity ratio of 49% during the first cycle. In spite of the fact that nanoparticles could have better capacity retention than their bulk analogues, the tendency to have a large irreversible capacity is a technical hurdle for achieving highly reversible anode materials.

In this study, we report an electrochemical comparison of $Sn_{87}Co_{13}$ alloys prepared by a normal $NaBH_4$ reduction method and a method using sodium naphthalenide as a reductant. Even though the method using sodium naphthalenide required an annealing process above 500 °C, the as-prepared sample

* Corresponding author. Tel.: +82 54 478 7824; fax: +82 54 478 7710.
E-mail address: jpcho@kumoh.ac.kr (J. Cho).

0013-4686/$ – see front matter © 2006 Elsevier Ltd. All rights reserved.
doi:10.1016/j.electacta.2006.11.033

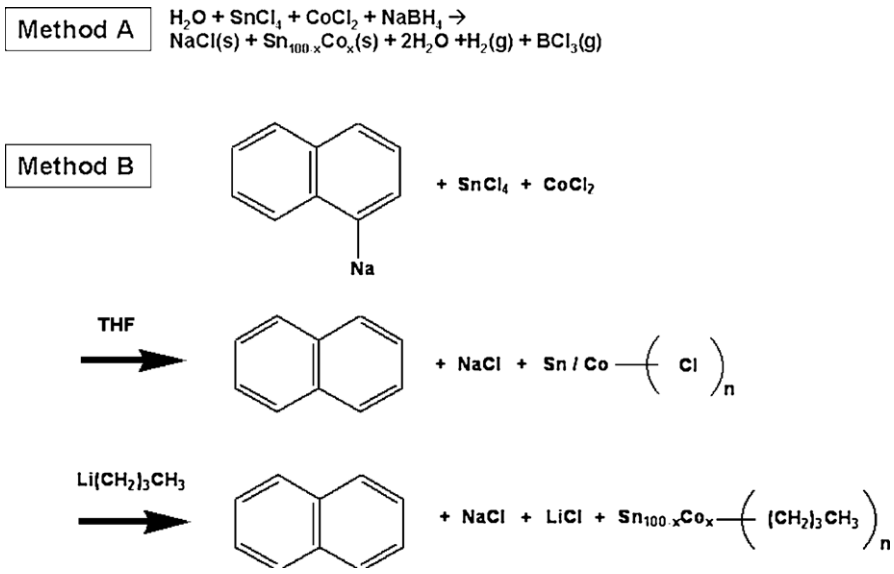

Fig. 1. Schematic diagrams of preparation methods A and B for $Sn_{87}Co_{13}$ alloys.

showed excellent capacity retention with a reversible capacity of 662 mAh/g and an irreversible capacity comparable to a bulk analogue.

2. Experimental

2.1. Synthesis

We used two different synthesis methods, one that did not utilize a surface terminating agent and other that used butyllithium as a surface terminating agent, to produce the nanoparticles. The first method (method A) consisted of the following steps. For $Sn_{87}Co_{13}$, 1.65 g of tetrammonium bromide was dissolved in 15 ml of CCl_4 while 0.845 g of $SnCl_2{\cdot}2H_2O$ (99.9%) and 0.297 g of $CoCl_2{\cdot}6H_2O$ (99.9%) were dissolved in 30 ml of distilled water. While stirring, 6 g of $NaBH_4$ that was previously dissolved in 15 ml of distilled water was slowly poured into the mixed solution. After stirring for 4 h, the solution was centrifuged, washed with distilled water to remove residual NaCl, rinsed with acetone, and vacuum-dried at 90 °C for 12 h to obtain $Sn_{87}Co_{13}$ nanoparticles.

The second method (method B) used a modified synthesis technique based on a procedure reported by Yang et al. [23]. In this method, 7.5 ml of anhydrous $SnCl_4$ (99.999%) and 0.5 g of $CoCl_2$ (99.99%) in a dried tetrahydrofuran were thoroughly mixed in a flask under a dry argon atmosphere in a glove box. This mixture was then poured into a solution consisting of 6 g of sodium metal and 14 g of naphthalene dissolved in 30 ml of tetrahydrofuran. This mixed solution was stirred for 24 h and then 60 ml of butyllithium (n-C_4H_9Li) was added. This solution was stirred at room temperature for 4 h with the solvent and naphthalene being removed by using a rotating evaporator at 90 °C. The product was washed with distilled water seven times and finally vacuum-dried at 120 °C for 48 h. The obtained product, which was a viscous liquid with a black color, was annealed at 700 °C for 5 h under a vacuum atmosphere.

The reaction diagrams for methods A and B are illustrated in Fig. 1, and both reactions led to the by-products LiCl and NaCl. A washing process using distilled water was essential. Chloride groups on the SnCo nanoparticles were replaced by C_4H_9 terminators, which eventually tuned into amorphous carbon at 700 °C.

2.2. Characterization

HRTEM samples were prepared by the evaporation of colloids in acetone or hexane on carbon-coated copper grids. The field-emission electron microscope was a JEOL 2000F operating at 200 kV. Powder X-ray diffraction measurements were carried out using a Rigaku D/Max2000 with a Cu-target tube. Inductively coupled plasma-mass spectroscopy (ICP, ICPS-1000IV, Shimadzu) was used to determine the metal contents. The carbon and hydrogen concentrations were measured using a CHNS analyzer (Flash EA 1112, Thermo Electron Corp.).

The electrochemical studies were carried out using coin-type half cells (2016 type) with a Li counter electrode. A $Sn_{87}Co_{13}$ alloy: PvdF binder: carbon black in a weight ratio of 8:1:1 was used as the working electrode.

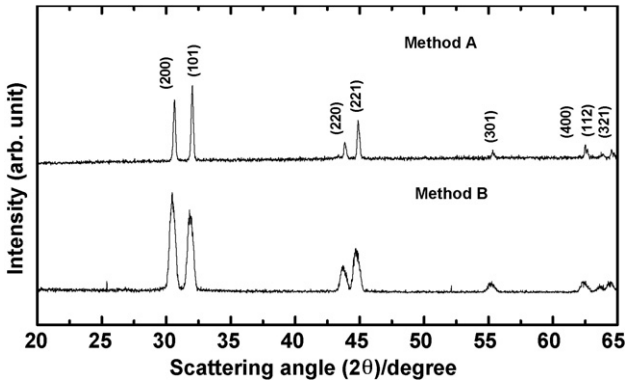

Fig. 2. XRD patterns of $Sn_{87}Co_{13}$ alloys prepared by methods A and B.

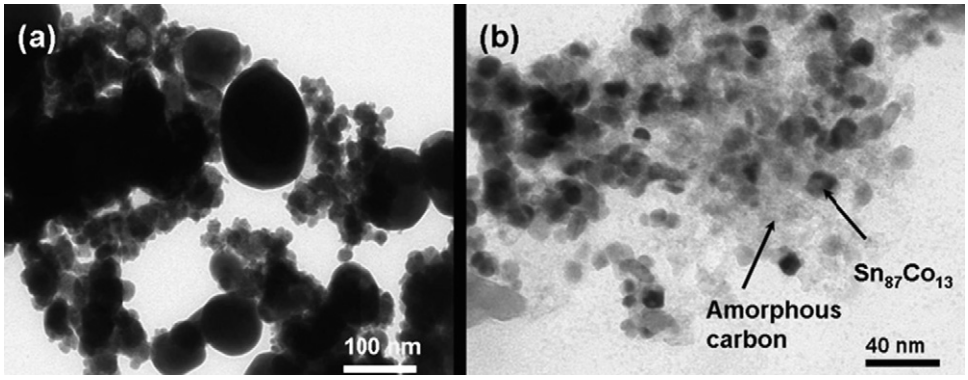

Fig. 3. TEM images of $Sn_{87}Co_{13}$ alloys prepared by methods A (a) and B (b).

3. Results and discussion

Fig. 2 shows the X-ray diffraction (XRD) patterns of $Sn_{87}Co_{13}$ nanoparticles prepared by methods A and B. Both powders had the β-Sn phase with no trace of Co peaks, indicating the formation of a solid solution without showing a $CoSn_2$ phase. This indicated that the Co atoms were completely incorporated into the Sn lattices. In nanoscale materials, supersaturated alloys can be formed without phase segregation, and, for example, 10 at.% Ni can be supersaturated into tetragonal tin [24]. Similarly, in a macroporous Sn–Co alloy, over 40 at.% Co was reported to be supersaturated in β-Sn lattices [25]. Accordingly, we believe that 13 at.% Co atoms can be substituted into Sn sites without phase segregation. Even though the melting temperature of pure β-Sn is ~200 °C, a 13 at.% addition of Co in β-Sn exhibits a melting temperature of above 800 °C in the phase diagram [26]. Fig. 3 shows transmission electron microscopy (TEM) images of the $Sn_{97}Co_{13}$ alloys prepared by methods A and B. The as-prepared sample using method A shows an irregular particle size distribution between 20 and 200 nm with some aggregation. The alloy prepared by method B exhibits relatively well-dispersed particles, with a size of 15 nm, that were covered by amorphous carbon. An inductively coupled plasma (ICP) analysis of the samples prepared by methods A

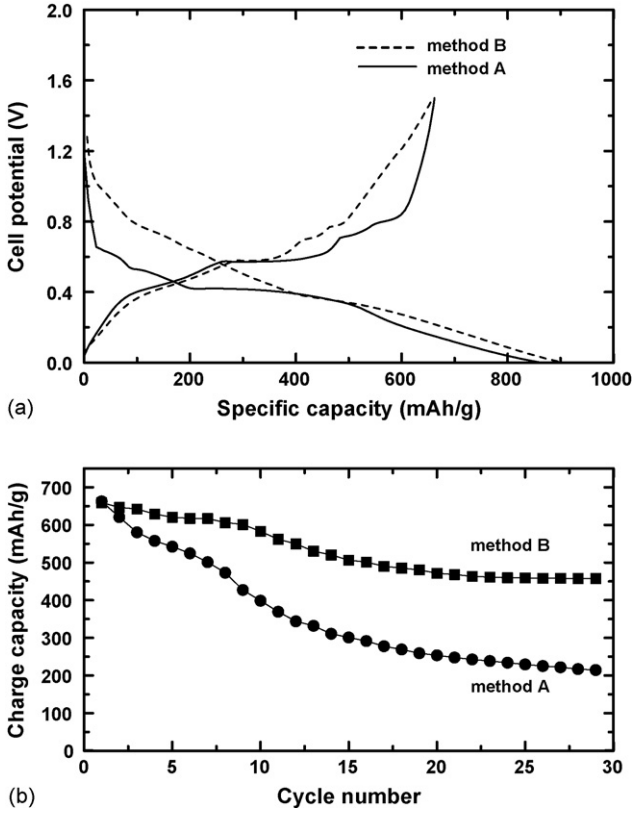

Fig. 4. Voltage profiles of the samples prepared by method A (a) and B (b) between 0 and 1.2 V at a rate of 0.2 C.

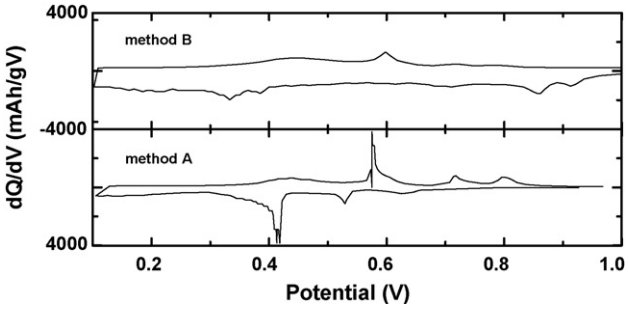

Fig. 5. Differential capacity as a function of potential for $Sn_{87}Co_{13}$ prepared by methods A and B during the first cycle.

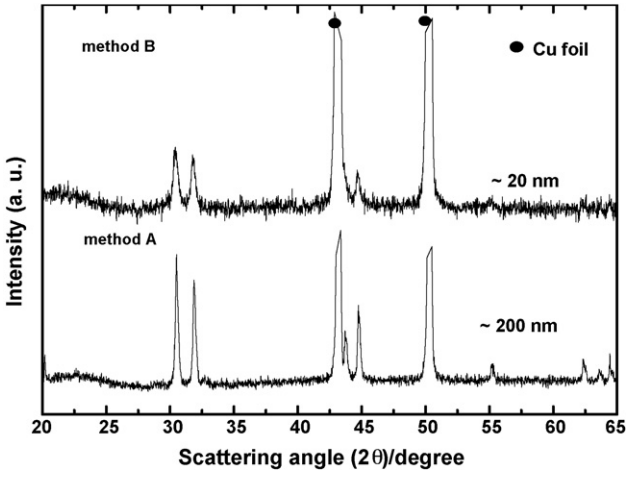

Fig. 6. XRD patterns of the samples prepared by methods A and B after 30 cycles.

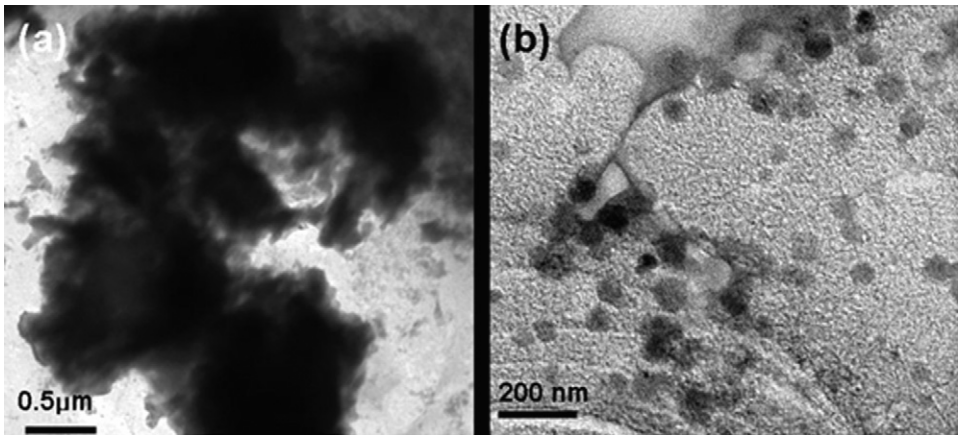

Fig. 7. TEM images of the samples prepared by methods A and B after 30 cycles.

and B confirmed the formation of $Sn_{86.5}Co_{12.5}$ and $Sn_{87.2}Co_{12.8}$, respectively. The amount of H and C in the sample prepared by method B was 0.01 and 10 wt.%, respectively, indicating that amorphous carbon contained a negligible amount of hydrogen after annealing at 700 °C. Fig. 4 shows voltage profiles of the samples prepared by both methods between 0 and 1.2 V at a rate of 0.2 C. First charge capacities for the samples prepared by method A and B were 658 mAh/g and 662 mAh/g, respectively, but the slightly larger irreversible capacity of the sample prepared by method B (13%) than that by method A (11%). The discharge capacity of 905 mAh/g (prepared by method B) during the first discharge agrees with the theoretical capacity of $Sn_{87}Co_{13}$ alloy, corresponding to was 900 mAh/g. Capacity contribution from the amorphous carbon was ~10 mAh/g [21]. However, the irreversible capacity of the sample prepared by method B is 3–4 times lower than other nanoalloys, which have an irreversible capacity of over 30% [1,17–19]. This indicated that the amorphous carbon layer effectively reduced side reactions. The capacity retention of the sample prepared using method B after 30 cycles was two times higher than that prepared by method A, which was 65%. Though the volume expansions of the metal hosts upon alloying with lithium are in the order of 300% large, absolute volume changes can be avoided when the size of the metallic host particles is kept small and uniform. In addition, the amorphous carbon layer can afford to provide a buffer zone for volume expansion.

Fig. 5 compares the differential capacity as a function of potential for $Sn_{87}Co_{13}$ prepared by methods A and B during the first cycle. The sample prepared by method A clearly shows peak growth between Li_xSn and Sn at 0.7 and 0.8 V, respectively, during the charge. In addition, sharp peaks between 0.4 and 0.6 V during discharge are indicative of the two phase transitions from Li_xSn to Sn. However, the $Sn_{87}Co_{13}$ electrode prepared by method B showed significantly depressed phase transitions as opposed to the samples prepared by method A. Considering that bulk sized Sn particles showed <10% capacity retention after 10 cycles [21], inactive Co atoms played a dominant role retarding the Sn aggregation. In accordance, possible reaction mechanism of $Sn_{87}Co_{13}$ can be written as:

$$Sn_{87}Co_{13} + xLi^+ + xe^- \leftrightarrow Li_xSn_{87}Co_{13}$$

Further evidence for a decrease in Sn particle growth can be seen in ex situ XRD patterns and TEM images after 30 cycles. Fig. 6 shows XRD patterns of the samples prepared by methods A and B after 30 cycles, and particle size can be estimated at 1 μm and 40 nm, respectively, using Debye-Scherr equation [27]. These values were 6.5 times and 4 times larger value than the initial particle size before cycling. This indicated that amorphous carbon layer acts as buffer layer for Sn particle aggregation during cycling. This result was consistent with TEM results that show the severely aggregated particle size of the sample prepared by method A in Fig. 7.

4. Conclusion

The $Sn_{87}Co_{13}$ nanoalloy prepared by using sodium naphthalene showed a reversible capacity of 658 mAh/g with a coulombic efficiency of 85% and demonstrated good capacity retention, compared with that prepared by using $NaBH_4$. The nanoalloys prepared by using sodium naphthalene showed improved dispersity and good coverage with amorphous carbon. Although, this procedure required an additional ligand exchange reaction with the grignard reagent, it led to easy control of particle size with and average size of <15 nm.

Acknowledgement

This work was supported by the Korea Research Foundation Grant funded by the Korean Government (MOEHRD, Basic Research Promotion Fund) (KRF-2006-003-C00162).

References

[1] J. Yang, M. Wachtler, S. Martin, J.O. Besenhard, Electrochem. Solid State Lett. 2 (1999) 161.
[2] M. Winter, J.O. Besenhard, Electrochim. Acta 45 (1999) 31.
[3] J. Graetz, C.C. Ahn, R. Yazami, B. Fultz, Electrochem. Solid State Lett. 6 (2003) A194.
[4] M.N. Obrovac, L. Christensen, Electrochem. Solid State Lett. 7 (2004) A93.
[5] H. Li, Q. Wang, L. Shi, L. Chen, X. Huang, Chem. Mater. 14 (2002) 103.
[6] H. Li, X. Haung, L. Chen, Z. Wu, Y. Liang, Electrochem. Solid State Lett. 2 (1999) 547.

[7] I.-S. Kim, G.E. Blomgren, P.N. Kumta, Electrochem. Solid State Lett. 7 (2004) A44.
[8] J.R. Dahn, R.E. Mar, A. Abouzeid, J. Electrochem. Soc. 153 (2006) A361.
[9] Y. Wang, J.Y. Lee, T.C. Deivaraj, J. Mater. Chem. 14 (2004) 2004.
[10] H. Uono, B.-C. Kim, T. Fuse, M. Ue, J.-I. Yamaki, J. Electrochem. Soc. 153 (2006) A1708.
[11] J. Yang, M. Winter, J.O. Besenhard, Solid State Ionics 90 (1996) 281.
[12] N. Dimov, S. Kugino, M. Yoshio, J. Power Sources 136 (2004) 108.
[13] I.-S Kim, P.N. Kumta, G.E. Blomgren, Electrochem. Solid State Lett. 3 (2000) 493.
[14] G.X. Wang, J. Yao, H.K. Liu, Electrochem. Solid State Lett. 7 (2004) A250.
[15] J. Yin, M. Wada, S. Tanase, T. Sakai, J. Electrochem. Soc. 151 (2004) A583.
[16] O. Mao, R.A. Dunlap, J.R. Dahn, J. Electrochem. Soc. 146 (1999) 405.
[17] J. Xie, X.B. Zhao, J.L. Mi, J. Tu, H.Y. Qin, G.S. Cao, J.P. Tu, Electrochem. Solid State Lett. 9 (2006) A336.
[18] J. Xie, X.B. Zhao, G.S. Cao, Y.D. Zhong, M.J. Zhao, J.P. Tu, Electrochim. Acta 50 (2005) 1903.
[19] M. Noh, Y. Kim, M.G. Kim, H. Lee, Y. Kwon, Y.Y. Lee, J. Cho, Chem. Mater. 17 (2005) 3320.
[20] Y. Kwon, M.G. Kim, Y. Kim, Y. Lee, J. Cho, Electrochem. Solid State Lett. 9 (2006) A34.
[21] M. Noh, Y. Kwon, H. Lee, J. Cho, Y. Kim, M.G. Kim, Chem. Mater. 17 (2005) 1926.
[22] Y. Wang, J.Y. Lee, T.C. Deivaraj, J. Electrochem. Soc. 151 (2004) A1804.
[23] C.-S. Yang, A. Bley, S.M. Kauzlarich, H.W.H. Lee, G.R. Delado, J. Am. Chem. Soc. 121 (1999) 5191.
[24] P. Villars, L.D. Calvert, Pearson's Handbook of Crystallographic Data for Intermetallic Phases, vol. 4, second ed., ASM International, Metals Park, OH, USA, 1991.
[25] Q. Lu, Z. Liu, L. Li, S. Xie, J. Kong, D. Zhao, Adv. Mater. 13 (2001) 286.
[26] T. Watanabe, Nanoplating: Microstructure Control Theory of Plated Film and Data Base of Plated Film Microstructure, Elsevier Publishers, Amsterdam, Netherlands, 2004.
[27] B.D. Cullity, Elements of X-ray Diffraction, second ed., Addison-Wesley, Menlo Park, USA, 1978.